RhoA-kinase coordinates F-actin organization and myosin II activity during semaphorin-3A-induced axon retraction

Gianluca Gallo

Drexel University College of Medicine, Department of Neurobiology and Anatomy, 2900 Queen Lane, Philadelphia, PA 19129, USA
e-mail: GGallo@drexelmed.edu

Summary

Axon guidance is mediated by the effects of attractant and repellent guidance cues on the cytoskeleton of growth cones and axons. During development, axon retraction is an important aspect of the pruning of inappropriately targeted axons in response to repellent guidance cues. I investigated the roles of RhoA-kinase and myosin II in semaphorin-3A-induced growth cone collapse and axon retraction. I report that semaphorin 3A activates myosin II in growth cones and axons. Myosin II activity is required for axon retraction but not growth cone collapse. Furthermore, semaphorin 3A promotes the formation of intra-axonal F-actin bundles in concert with the loss of F-actin in growth cone lamellipodia and filopodia. Formation of axonal F-actin bundles was independent of myosin II, but partially required RhoA-kinase activity. Conversely, RhoA-kinase activity was required to shut down F-actin polymerization underlying protrusive activity. Collectively, these observations suggest that guidance cues cause axon retraction through the coordinated activation of myosin II and the formation of intra-axonal F-actin bundles for myosin-II-based force generation. I suggest that in the context of semaphorin 3A signaling, RhoA-kinase serves as a switch to change the function of the F-actin cytoskeleton from promoting protrusive activity to generating contractile forces.

Key words: RhoA, RhoA-kinase, Cellular contractility, Axon guidance, Growth cone collapse, Cytoskeleton

Introduction

Axons are guided to their targets by a variety of extracellular guidance cues (Plachez and Richards, 2005). Guidance cues activate signaling transduction pathways that, in turn, regulate the dynamics and organization of the neuronal cytoskeleton. Guidance cues can steer growth cones towards or away from the source of the cue. Repellent guidance cues induce growth cone collapse, characterized by the loss of protrusive lamellipodia and filopodia (Gallo and Letourneau, 2004). Growth cone collapse is often followed by axon retraction. Axon retraction induced by guidance cues is of fundamental importance during refinement of axonal projections (reviewed in Luo and O'Leary, 2005). Although the role of axon retraction during development of the nervous system is well appreciated, the mechanism of guidance-cue-induced retraction is not fully elucidated.

A requirement for actin filaments (F-actin) in mediating axon retraction has long been established (Solomon and Magendantz, 1981). Similarly, previous studies identified myosin II as an essential component of the mechanism of axon retraction in response to repellent guidance cues (Wylie and Chantler, 2003; Gallo et al., 2002), axotomy (Gallo, 2004), stabilization of the actin cytoskeleton (Gallo et al., 2002), and inhibition of microtubule motors (Ahmad et al., 2000). Myosin II interacts with F-actin to generate contractile forces that result in axon retraction. Although myosin II is found throughout axons and growth cones (Rochlin et al., 1995), F-actin is concentrated at the growth cone and sparse in the axon (Letourneau, 1983). Importantly, repellent guidance cues cause growth cone collapse and depolymerize growth cone F-actin while promoting axon retraction (Gallo and Letourneau, 2004). The dependence of axon retraction on myosin II activity and F-actin thus raises a paradox; how can myosin II drive axon retraction if the major source of the required substratum for force generation, growth cone F-actin, has been depleted?

In cells, F-actin assumes specific types of organization depending on its functions. Neurons exhibit two types of protrusive structures, lamellipodia and filopodia, each supported by a different type of F-actin organization (Gallo and Letourneau, 2004). In lamellipodia, actin filaments form meshworks that drive lamellipodial advance. In filopodia, actin filaments are arranged as bundles of filaments. The polymerization of filaments at the leading edge of lamellipodia and filopodia drives the protrusion of these structures. Actin filaments also serve contractile functions through their association with myosin II. Actin filaments in contractile structures, such as stress fibers, sarcomeres or cytokinetic rings, are organized as intracellular bundles of aligned filaments (Maupin and Pollard, 1986; Burridge and Chrzanowska-Wodnicka, 1996). Contractile forces are then generated by the activity of myosin II, pulling on these filaments (Straight et al., 2003). The F-actin substrata for myosin-II-dependent force generation during axon retraction have not been identified. In this report I demonstrate that the growth-cone-collapse- and axon-retraction-inducing guidance cue semaphorin 3A causes a loss of F-actin that drives

protrusive structures but generates an intra-axonal system of F-actin bundles that serve as the substratum for myosin-II-driven axon retraction.

Results

Myosin II activity is required for semaphorin-3A-induced axon retraction but not growth cone collapse

The upstream regulators of myosin II, RhoA and RhoA-kinase (ROCK), have been shown to be signaling intermediates when it comes to guidance cues, including ephrins and semaphorin 3A, that induce growth cone collapse and axon retraction (Wahl et al., 2000; Hall et al., 2001; Hu et al., 2001; Gallo et al., 2002; Swiercz et al., 2002; Dontchev and Letourneau, 2002; Wu et al., 2005). ROCK positively regulates the activity of myosin II by increasing the phosphorylation of myosin II regulatory light chains (Ueda et al., 2002). However, ROCK regulates additional pathways that might be involved in axon retraction and growth cone collapse (e.g. LIM-kinase and cofilin) (Aizawa et al., 2001). To determine the role of myosin II downstream of semaphorin 3A, I inhibited myosin II activity by using blebbistatin (at 50 μM), a specific inhibitor of myosin IIA and IIB (Straight et al., 2003; Gallo, 2004; Gehler et al., 2004; Loudon et al., 2006) and treated cultures with semaphorin 3A.

Time-lapse phase-contrast imaging revealed that treatment with semaphorin 3A induced growth cone collapse and axon retraction (Fig. 1A). Growth cones collapsed between 3 and 12 minutes after treatment. Axon retraction commenced once all protrusive activity of the growth cone had ceased. Following treatment with semaphorin 3A, 87% of axons (n=23) underwent net retraction and 13% of axons failed to retract and stalled, exhibiting neither retraction nor extension. Consistent with the report of Turney and Bridgman (Turney and Bridgman, 2005), treatment of axons growing on a laminin substratum with blebbistatin alone decreased the axon extension rate by approximately 40% (Fig. 1B). Quantitative determination of the distance axons retracted following semaphorin 3A treatment revealed that, inhibition of myosin II with blebbistatin decreased the distance axons underwent retraction by 85% (Fig. 1B). In the presence of blebbistatin, following treatment with semaphorin 3A, 77% of axons stalled and 23% underwent minor retraction (n=31).

We next investigated whether inhibition of the RhoA–ROCK–myosin-II regulatory pathway could block axon retraction in response to semaphorin 3A. Inhibition of ROCK with 10 μM y-27632 or Chariot-peptide-mediated transfection with C3 toxin to block RhoA, blocked axon retraction (Fig. 1B,D). However, unlike following inhibition of myosin II using blebbistatin, when RhoA-ROCK signaling was inhibited, axons continued to extend after treatment with semaphorin 3A. Following semaphorin 3A treatment, the mean rate of axon extension in the presence of y-27632 was 36% slower than in cultures treated with y-27632 alone (Fig. 1B). Similarly, following treatment with semaphorin 3A, the mean rate of axon extension in C3-transfected axons was 30% slower than in controls transfected with C3 without semaphorin 3A treatment (Fig. 1B). A similar percent decrease in the mean axon extension rate following semaphorin 3A treatment was observed with both y-27632 and C3 pretreatment, but neither of these differences reached statistical significance (P>0.09 and P>0.15, respectively). Thus, although semaphorin 3A

treatment in the presence of y-27632 or C3 slightly attenuated the rate of axon extension, axons continued to extend. Collectively, these data indicate that myosin II acts downstream of ROCK during semaphorin-3A-induced axon retraction. Moreover, these results suggest that myosin-II-independent mechanisms downstream of RhoA-ROCK block the ability of axons to extend following treatment with semaphorin 3A.

A report by Kolega has revealed that illumination of blebbistatin with light of 365 nm or 450-490 nm wavelengths can result in phototoxic effects (Kolega, 2004). Control experiments on the effects of blebbistatin on axon retraction in the absence of phase-contrast live imaging and illumination ruled out possible illumination-related confounds. Briefly, cultures were treated with blebbistatin or DMSO without illumination. Next, a picture was acquired just prior to treatment with semaphorin 3A, another 30 minutes after treatment – without intervening illumination. Under these conditions control axons treated with semaphorin retracted 27±6 μm (n=22), whereas blebbistatin-treated axons retracted only 7±4 μm (n=28), similar to the effects of blebbistatin in the live-imaging experiments presented in Fig. 1.

A role of RhoA-ROCK signaling in mediating growth cone collapse in response to semaphorins and ephrins has been previously demonstrated (Wahl et al., 2000; Dontchev and Letourneau, 2002; Dontchev and Letourneau, 2003; Gallo and Letourneau, 2004). Given that myosin II is an effector of ROCK, myosin II has been proposed to act downstream of repellent guidance cues leading to growth cone collapse (Wahl et al., 2000; Gallo and Letourneau, 2004). Inhibition of ROCK with y-27632 or C3 to block RhoA, partially decreased the extent of semaphorin-3A-induced growth cone collapse (Fig. 1C). The percentage of collapsed growth cones in response to semaphorin 3A decreased by 68% and 77%, respectively, following y-27632 and C3 pretreatment relative to semaphorin 3A treatment alone (Fig. 1C). Thus, although semaphorin-3A-induced growth cone collapse was decreased by inhibition of RhoA or ROCK, the effect was not complete. Partial inhibition of growth cone collapse in response to semaphorin 3A is consistent with previous studies (Dontchev and Letourneau, 2002). In contrast to inhibition of RhoA or ROCK, treatment with blebbistatin to inhibit myosin II did not alter the percentage of growth cones collapsed after treatment with semaphorin 3A (Fig. 1A,C). Thus, semaphorin-3A-induced axon retraction but not growth cone collapse requires myosin II activity downstream of ROCK.

Semaphorin 3A increases axonal F-actin levels by inducing intra-axonal F-actin bundles

Axon retraction requires F-actin, but semaphorin 3A causes growth cone collapse and thus the loss of the largest source of F-actin available for myosin II to drive axonal contractility during retraction (Letourneau, 1983). This consideration raises the question of the source of F-actin that myosin II uses to drive axon retraction in response to semaphorin 3A. To determine the effects of semaphorin 3A on the organization of F-actin in growth cones and axons, I investigated the amount and organization of F-actin at the growth cone and along the axon following semaphorin 3A treatment. In control axons F-actin accumulates at the growth cone, sparsely in the distal 20 μm of axons, and at relatively lower levels in the more proximal
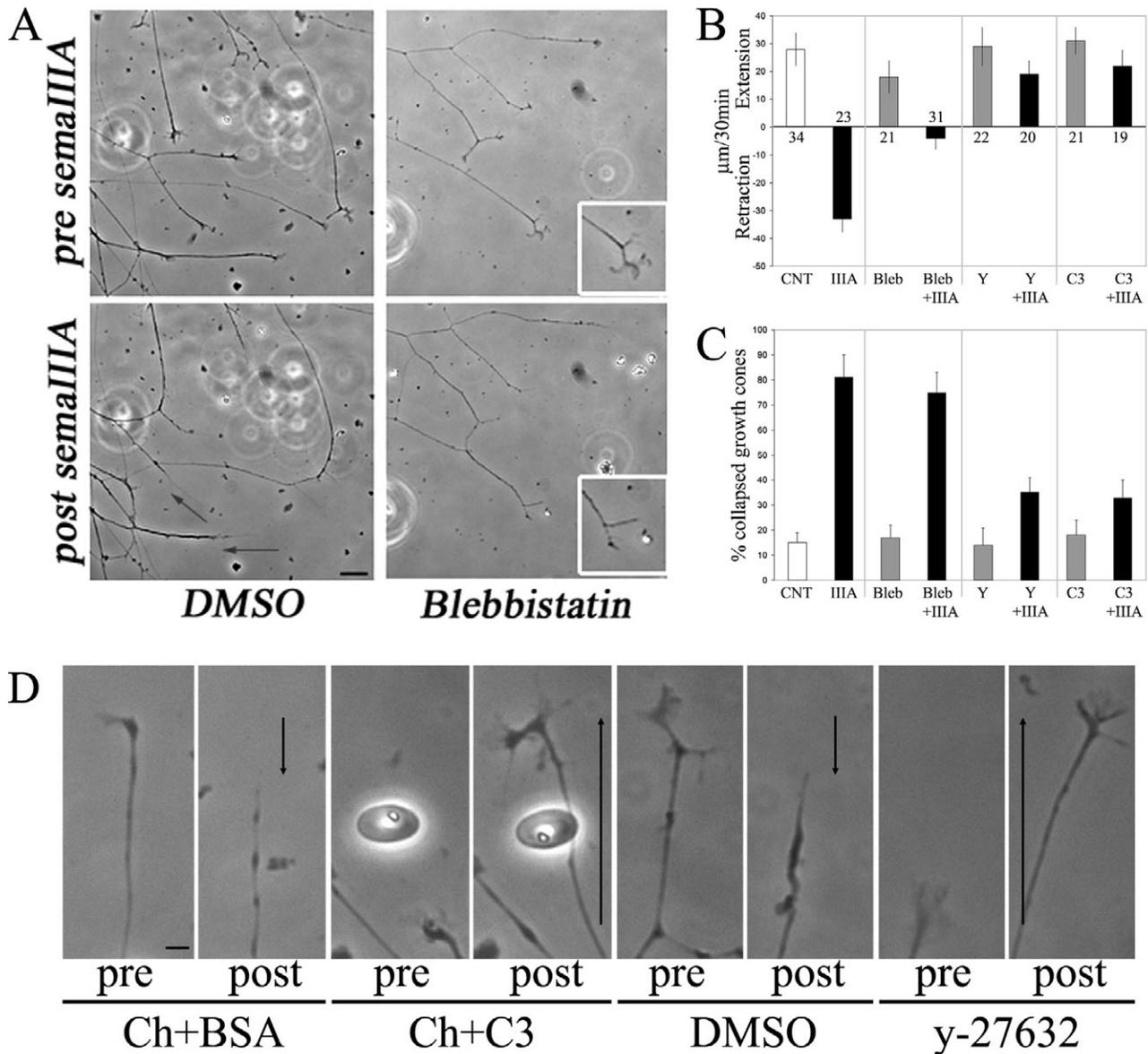
Fig. 1. Myosin II blocks semaphoring-3A-induced axon retraction but not growth cone collapse. (A) Still images from time-lapse sequences of the responses of axons to treatment with semaphorin 3A (SemaIIIA) or semaphorin 3A with blebbistatin pretreatment (50 µM, 1 hour). Controls were treated with DMSO, the vehicle for blebbistatin. Images of the same axons before (top panels) and 30 minutes after (bottom panels) treatment with semaphorin 3A. Treatment with semaphorin 3A caused growth cone collapse and axon retraction (arrows denote extent of retraction). Insets in blebbistatin-treated culture show a higher magnification view of the adjacent growth cone. Note that, in the presence of blebbistatin and after semaphorin 3A treatment, growth cones collapse but axons do not retract. Bar, 20 µm. (B) Quantification of the mean extension-retraction rates of axons pretreated with either 50 µM blebbistatin (Bleb), 10 µM y-27632 (Y) or transfected with 1 µg C3 (C3) by using Chariot with or without semaphorin 3A (IIIA) treatment. The control group for blebbistatin treatment alone (CNT) was treated with BSA. Relative to the CNT group, semaphorin 3A treatment induced strong axon retraction ($P<0.0001$). Blebbistatin inhibited semaphorin-3-A-induced retraction ($P<0.003$, Bleb+IIIA versus IIIA). Pretreatment with Y or C3 also blocked retraction ($P<0.0001$ for both comparisons, Y+ IIIA and C3+IIIA versus IIIA). Neither Y nor C3 treatment altered axon extension rate relative to CNT ($P>0.7$ for both comparisons). Blebbistatin decreased axon extension rate relative to CNT ($P<0.03$). Numbers above or below bars represent the number of axons measured (n). (C) DRG explants were treated for 30 minutes with semaphorin 3A following pretreatment with Blebbistatin, y-27632 or C3. Fixed cultures were stained with Rhodamine-phalloidin and the percentage of collapsed growth cones determined blind of treatment. No statistically significant differences were observed in comparisons of blebbistatin with CNT, or IIIA relative to bleb+IIIA. Neither Y nor C3 treatment altered growth cone collapse relative to CNT or treatment with Chariot and BSA (data not shown). Both Y and C3 treatment decreased the percentage of growth cones that collapsed after treatment with semaphorin 3A ($P<0.001$ for both comparisons). However, in both Y- and C3-treated groups, semaphorin 3A slightly increased the percentage of collapsed growth cones relative to Y or C3 treatment alone ($P<0.02$ or $P<0.03$, respectively). Means were obtained from 10-15 cultures per group with 80-100 growth cones scored per culture. Welch t-test was used for comparisons. (D) Responses of axons pretreated with either C3 or y-27632 to treatment with semaphorin 3A. Images are shown before (pre) and 30 minutes after (post) treatment with semaphorin 3A. Ch, chariot. Arrows denote axon extension (upwards arrow) or retraction (downwards arrow). Bar, 10 µm.

axon shaft (Fig. 2A). Following treatment with semaphorin 3A F-actin levels at the tip of axons were greatly decreased and lamellipodia and filopodia had undergone collapse, as expected from previous reports focusing on the F-actin content in the distal-most extent of the axon (reviewed in Gallo and Letourneau, 2004). However, after treatment with semaphorin 3A F-actin levels increased throughout the distal 100 μm of axons (Fig. 2A), a part of the axon behind the growth cone that does not normally exhibit high levels of F-actin. Quantification of F-actin staining revealed a time-dependent increase in axons following semaphorin 3A treatment that reached a plateau of 65-75% increase relative to time-matched controls by 10 minutes after treatment ($P<0.01$, $n>30$ per time point, 0, 5, 10, 15, 20 and 30 minutes after treatment, n=25-30 axons per group). F-actin in semaphorin-A-treated axons was organized in the form of intra-axonal bundles that generally extended parallel to the axis of the axon (Fig. 2B). However, the F-actin bundles often appeared to cross from one side of axons to the other (Fig. 2B). Thus, semaphorin 3A induced an intra-axonal cage-like organization of F-actin bundles in axons.

Given that semaphorin 3A induced a cage-like organization of F-actin, which could serve as a substratum for myosin II to generate contractile forces during axon retraction, I sought

to determine whether myosin II underwent detectable redistributions in axons following semaphorin 3A treatment. To investigate the distributions of axonal F-actin bundles and myosin II after treatment with semaphorin 3A, I double labeled axons with phalloidin and antibodies specific to myosin IIA and IIB (Fig. 2C). In control axons, both myosin isoforms are present in a uniform punctuate distribution, presumably reflective of myosin II mini-filament formation (Bridgman, 2002). Axonal F-actin bundles induced by semaphorin 3A were invariably colocalized with myosin II in the axon (Fig. 2C). Sideward buckling of the axonal shaft is a common feature of retracting axons (Luo and O'Leary, 2005). Interestingly, at sites of axonal buckling I observed accumulations of myosin IIA (Fig. 2C), perhaps reflective of regions of greater myosin II force generation resulting in a distortion of the axon shaft. Similarly, myosin IIA was often concentrated at the tip of retracting axons (Fig. 2C). Myosin IIB did not appear to exhibit similar concentrations at sites of axonal buckling and retracting axon tips (Fig. 2C). Moreover, the staining intensity of myosin IIB was lower than that of myosin IIA in both control and semaphorin-3A-treated axons. Thus, the relative distribution of myosin IIA is consistent with the proposed role of myosin IIA in driving axon retraction (Wylie and Chantler, 2003). The
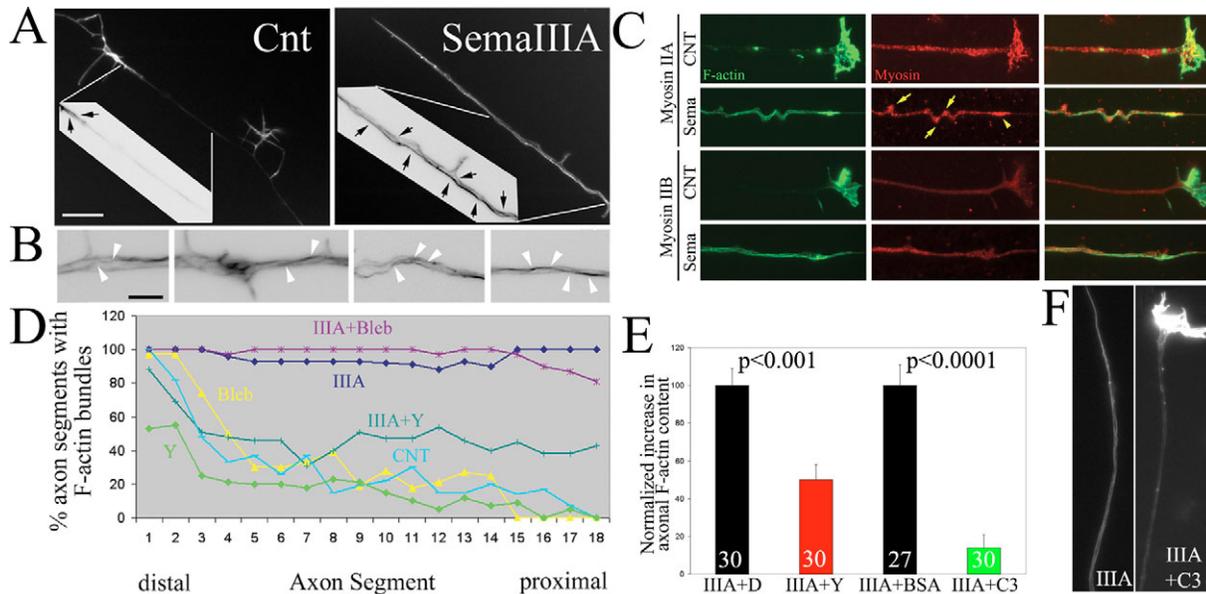

Fig. 2. Semaphorin 3A induces axonal F-actin bundles. (A) Control (CNT) axons exhibit F-actin staining restricted to the distal axon (arrows in color-inverted inset). Semaphorin 3A (SemaIIIA) treatment increased phalloidin staining relative to control axons and induced F-actin bundles throughout the axon (arrows in inset). Bar,10 μm. (B) Four panels showing details of semaphorin-3A-induced axonal F-actin bundles (images were color inverted). Arrowheads denote what appear to be continuous F-actin bundles that cross from one side of the axon to the other. Bar, 2 μm. (C) Examples of axons double labeled with phalloidin and myosin-II-isoform-specific antibodies. Axons were treated for 20 minutes with either semaphorin 3A (Sema) or BSA as a control (CNT) prior to fixation. Note colocalization of myosin IIA aggregates with areas of axonal buckling (yellow arrows) and at the tip of the retracting axon (yellow arrowhead). I did not observe a similar organization of myosin IIB in semaphorin-3A-treated axons, in which myosin IIB distribution appeared relatively uniform. (D) Quantification of the percentage of axons that exhibit F-actin bundles as a function of distance from the tip of the axon in 5 μm bins. Control axons (CNT) reliably (>50%) exhibited bundles only in the distal-most 20 μm. Semaphorin 3A treatment for 30 minutes (IIIA) induced axon F-actin bundles up to 100 μm behind the growth cone. Blebbistatin (Bleb) did not alter semaphorin 3A induction of bundles. y-27632 at 10 μM (Y) partially decreased semaphorin-3A-induced formation of axon bundles. Thirty axons were measured per group. (E) Increase in axonal F-actin content relative to controls not treated with semaphorin 3A. Controls were treated with DMSO or transfected with BSA, for y-27632 (10 μM) and C3 transfection, respectively. Numbers indicate n of axons measured. (F) Examples of axons transfected with BSA or C3 and then treated with semaphorin 3A and stained with phalloidin to reveal F-actin. Note that the C3-transfected axon retrained the growth cone and did not develop prominent axonal F-actin bundles following treatment with semaphorin 3A (IIIA+C3, right panel).

functional significance of the accumulation of myosin IIA in my system will require further investigation, but demonstrates that myosin IIA redistributes during axon retraction.

ROCK activity drives the formation of cytoplasmic F-actin bundles in non-neuronal cells (Yoneda et al., 2005) and in the central domains of growth cones (Loudon et al., 2006). I therefore investigated whether RhoA and ROCK activity is required for semaphorin-3A-induced F-actin bundles. The increase in F-actin levels in axons following semaphorin 3A treatment was decreased by 50% in the presence of the ROCK inhibitor y-27632 (10 μM; Fig. 2E). To determine whether ROCK inhibition affected semaphorin-3A-induced axonal bundles, I performed a blind semi-quantitative analysis of the presence of F-actin bundle structures in axons. Axons were subdivided into 5-μm segments and scored for the presence of bundles. The percentage of axon segments exhibiting bundles as a function of distance from the tip of the axon was depicted in a graph (Fig. 2D). Control axons consistently exhibited bundles only in the distal 20 μm (Fig. 2A, arrows in inset). However, following semaphorin 3A treatment, bundles were present throughout the distal 100 μm of axons. Consistent with measurements of total F-actin levels in axons, y-27632 treatment decreased the percentage of axonal segments exhibiting bundles by approximately 50% (Fig. 2D). y-27632 treatment also decreased the exhibition of bundles in the distal 20 μm of axons treated with the ROCK inhibitor alone (Fig. 2D).

Similar to the inhibition of ROCK, inhibition of RhoA by using C3 toxin decreased the exhibition of F-actin bundles following semaphorin 3A treatment (Fig. 2F). However, the effect of direct RhoA inhibition on axonal bundles was more pronounced than that of inhibition of ROCK. C3 pretreatment reduced the axonal F-actin content that had been induced by semaphorin 3A by approximately 86% (Fig. 2E,F). Thus, RhoA activity is required for the formation and/or maintenance of intra-axonal F-actin bundles in response to semaphorin 3A. Inhibition of RhoA had a more pronounced effect than inhibition of ROCK on semaphorin 3A-induced bundles. This discrepancy indicates that, in the context of semaphorin 3A signaling, downstream effectors of RhoA other than ROCK (e.g. mDia1) also contribute to bundle formation and/or maintenance (Watanabe et al., 1999). The greater effect of C3 on axonal F-actin-bundle formation relative to treatment with 10 μM y-27632 is probably not due to this dose of y-27632 being sub-optimal because we have previously determined that it decreases the endogenous levels of regulatory myosin light chain phosphorylation by approximately 80% (Loudon et al., 2006) and blocks semaphorin-3A-induced increases in the phosphorylation of regulatory myosin light chain (Fig. 4C).

Myosin II activity has been reported to be required for the formation or maintenance of some forms of F-actin bundles (Bridgman et al., 2001; Guha et al., 2005). However, inhibition of myosin II by using blebbistatin did not alter the semaphorin-3A-induced increase in axonal F-actin content ($P>0.05$) or the exhibition of axonal bundles (Fig. 2D). Thus, myosin II activity downstream of ROCK is not required for semaphoring-3A-induced axonal F-actin bundles.

RhoA activation of ROCK is sufficient to induce axonal F-actin bundles

RhoA is activated by semaphorin signaling and, in turn, activates ROCK (Hall et al., 2001; Hu et al., 2001; Swiercz et al., 2002; Dontchev and Letourneau, 2002; Wu et al., 2005). The activation of RhoA-ROCK by semaphorin 3A is required for the formation or maintenance of axonal F-actin bundles (Fig. 2). I next determined whether activation of ROCK by RhoA is sufficient to explain the effects of semaphorin 3A on the formation of axonal F-actin bundles. To determine whether RhoA-ROCK activity alone is sufficient for the formation of axonal F-actin bundles, I transfected neurons with constitutively active RhoA protein (L63RhoA) using the peptide carrier Chariot (reviewed in Gallo, 2003). Three hours after transfection, 57% of L63RhoA-transfected growth cones were fully collapsed, compared with only 16% in BSA-transfected control cultures ($n>100$ growth cones in each group). Examination of the F-actin cytoskeleton revealed that L63RhoA-transfected axons exhibited intra-axonal F-actin bundles that were not qualitatively distinguishable from semaphorin-3A-induced F-actin bundles (Fig. 3A). Axonal F-actin bundles were also observed in axons that exhibited only partially collapsed growth cones (Fig. 3B). Bundles were localized parallel to the axis of the axon and also crossed over from one side to the other (Fig. 3A,B, see insets), similar to bundles formed in response to semaphorin 3A (Fig. 2). L63RhoA increased the axonal F-actin content by 60% relative to BSA controls ($P<0.01$, $n=30$ axons per group). No difference in F-actin content was detected in axons treated with y-27632 or y-27632 together with L63RhoA ($P>0.7$, $n=30$ axons per group). Analysis of the distribution of axonal F-actin bundles revealed no differences of axons treated with y-27632 or y-27632 together with L63RhoA treated axons (Fig. 3C). Thus, although constitutively active RhoA can promote F-actin-bundle formation that strictly depends on ROCK, semaphorin 3A might activate additional parallel pathways that can partially compensate for lack of ROCK activity. Alternatively, the degree of L63RhoA transfection might not attain the same levels of high RhoA activity induced by semaphorin 3A. In this case then the same concentration of y-27632 (10 μM) may have a greater effect on bundles formed in response to L63RhoA compared with semaphorin 3A. Regardless, these data demonstrate that ROCK, downstream of RhoA, is sufficient to induce axonal F-actin-bundle formation.

### Loading of constitutively active RhoA into axons induces axon retraction

Similar to the effects of semaphorin 3A, L63RhoA caused growth cone collapse and the formation of axonal F-actin bundles in axons. I next determined whether L63RhoA, like semaphorin 3A, also induced axon retraction in conjunction with growth cone collapse and the formation of axonal F-actin bundles. L63RhoA-transfected axons grew at a slower rate and underwent more frequent spontaneous retraction than control axons transfected with BSA. Cultures were transfected for 2 hours before imaging experiments. To prevent sampling bias, all axons in the field were counted in the analysis, regardless of whether the growth cone was collapsed or not. L63RhoA transfection decreased during the time that axons spent actively elongating by 81% relative to transfections with BSA ($P<0.000001$; Fig. 3D). During a 40-minute imaging period, L63RhoA-transfected axons extended 6.5±1.1 minutes ($n=30$) during observation, compared with 34.9±0.9 minutes ($n=25$) for BSA-transfected axons. L63RhoA-transfected axons that

Fig. 3. Constitutively active RhoA-induced RhoA-kinase-dependent axonal F-actin bundles. (A,B) Chariot-peptide-mediated transfection of axons with constitutively active RhoA (L63RhoA) induced axon bundles in axons that (A) underwent retractions and also in axons that (B) did not retract but exhibited partially collapsed growth cones with distal accumulation of F-actin. Insets show magnified and color-inverted regions of the axons as denoted by the white lines. Bar, 10 µm. (C) Quantification (in percent) of axon segments exhibiting F-actin bundles (as shown in Fig. 2) revealed that treatment with y-27632 at the time of L63RhoA transfection completely inhibited the formation of F-actin bundles. (D) L63RhoA decreased the percentage of time that axon spent extending relative to BSA-treated controls. Data are normalized to BSA-transfected axons. (E) Inhibition of ROCK minimized L63RhoA-induced axon retraction. The percentage of axons simultaneously transfected with L63RhoA and treated with y-27632 that exhibit retraction during imaging was decreased by 69% relative to axons transfected with L63RhoA.
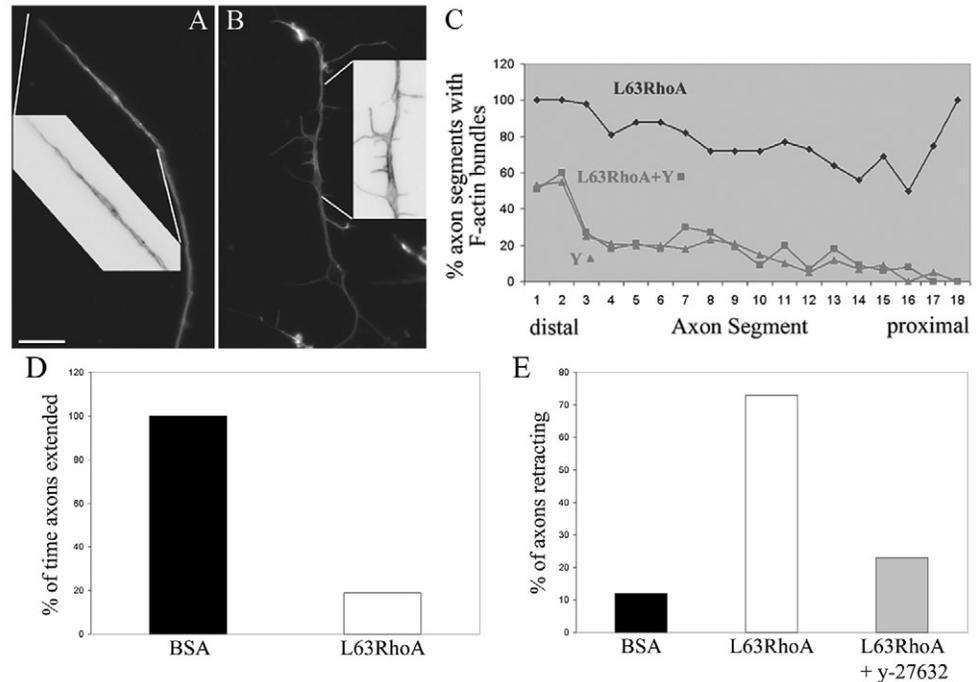
did not extend, either stalled or retracted. Stalling was defined as the period were the tip of the axon neither advanced nor retracted. During a 40-minute imaging period 12% and 73% of BSA- and L63RhoA-transfected axons, respectively, underwent retraction for ⩾3 minutes (Fig. 3E). The mean time individual control axons spent retracting during a bout of retraction was 2.0±0.6 minutes ($n=3$ axons) in BSA-transfected controls. Control BSA-transfected axons were observed to retract at a maximum of 3 minutes during imaging. L63RhoA increased the time axons spent retracting during a bout of retraction by 200% (6.0±0.7 minutes; $n=30$ axons, $P<0.001$, Welch t-test). In addition, three of the L63RhoA-transfected axons underwent a net retraction of 17±2 µm/40 minute. None of the control axons underwent net retraction. Thus, the introduction of L63RhoA alone is sufficient to promote axon retraction, inhibit axon extension rate and induce axonal F-actin bundles.

To determine the role of ROCK in the inhibitory effects of L63RhoA on axon extension, axons were treated with y-27632 at the time of transfection and compared with L63RhoA-transfected axons. Co-treatment with y-27632 partially reversed the inhibition of axon extension rate induced by L63RhoA. y-27632 treated L63RhoA transfected axons extended at 44% the rate of control y-27632 treated BSA-transfected axons, relative to 13% for axons transfected with L63RhoA alone ($P<0.001$). Axons treated simultaneously with L63RhoA and y-27632 exhibited an increase in the time spent elongating compared with axons treated with L63RhoA alone (9.7±0.9 compared with 6.5±1.1 minutes, respectively, $P<0.03$ Welch t-test). The time axons spent stalling did not differ between the two groups ($P>0.1$, Welch t-test).

To determine the contribution of ROCK to the axon-retraction-induced L63RhoA, I determined the percentage of

axons retracting in cultures that had been transfected with L63RhoA and simultaneously treated with 10 µM y-27632. Determination of the percentage of retracting axons in a time period above the maximum for control axons (3 minutes) yielded 73% for L63RhoA-transfected axons and 23% for axons transfected with L63RhoA and treated with y-27632 at the same time ($n=32$; Fig. 3E). In addition, the mean time spent in a bout of retraction by L63RhoA-transfected axons treated with y-27632 and by BSA-transfected controls was the same (2.7±0.5 minutes, $n=12$ and 2.0±0.6 minutes, $n=3$, respectively) ($P>0.4$, Welch t-test), compared with the 200% increase compared with controls induced by transfection with L63RhoA alone.

Collectively these data demonstrate that ROCK, downstream of L63RhoA, induces axon retraction and inhibits forward extension of the axon. Axon stalling may be mediated by additional components of the RhoA pathway, or reflect insufficient net RhoA activity to fully drive retraction. Overall, these data are consistent with RhoA-ROCK activity mediating axon retraction downstream of semaphorin 3A signaling.

ROCK is required for semaphorin-3A-induced activation of myosin II in axons

Although myosin II has been shown to be required for retraction, few studies have determined the state of myosin II activation in relation to treatment with repellent guidance cues (Wahl et al., 2000; Alabed et al., 2006). This determination is important because endogenous myosin II activity is sufficient to drive retraction in response to pharmacological stabilization of the actin cytoskeleton (Gallo et al., 2002). Therefore, I first asked whether semaphorin 3A activates myosin II in the axons of nerve growth factor (NGF)-responsive embryonic dorsal root ganglion cultures. Myosin II activation depends on

phosphorylation of serine residue 19 of the regulatory myosin light chains (rMLC) (Bresnick, 1999) by kinases, including RhoA-kinase. I used an antibody specific to rMLC phosphorylated on serine 19 to stain axons before and after treatment with semaphorin 3A, as previously reported (Loudon et al., 2006). The intensity of phosphorylated rMLC staining was expressed as the ratio to the intensity of a volumetric marker (CellTracker, see Materials and Methods). The activation of myosin II was determined 10 minutes post treatment because at this time, growth cones have collapsed and axons have begun retracting. Treatment with semaphorin 3A increased myosin II activity above control levels (Fig. 4A,B). These data demonstrate that myosin II is an active component of the semaphorin 3A signaling cascade.

To determine whether ROCK activity is required for semaphorin-3A-induced increases in rMLC phosphorylation, cultures were treated with y-27632 before treatment with semaphorin 3A. In the presence of 10 μM y-27632, semaphorin 3A failed to elevate rMLC phosphorylation levels above the levels present in axons treated with y-27632 alone (Fig. 4C). Thus, ROCK signaling is required for the activation of myosin II by semaphorin 3A.

Inhibition of ROCK prevents a semaphorin-3A-induced block of F-actin polymerization that leads to protrusive activity

Inhibition of ROCK decreases growth cone collapse and axon retraction in response to semaphorin 3A (Fig. 1) (Dontchev and Letourneau, 2002; Dontchev and Letourneau, 2003). However, myosin II is required for semaphorin-3A-induced axon retraction but not growth cone collapse (see Fig. 1). The hallmark of growth cone collapse is the loss of growth cone F-actin, which supports the formation of lamellipodia and filopodia (Gallo and Letourneau, 2004). I therefore tested whether ROCK mediates the effects of semaphorin 3A on F-actin polymerization in growth cones that leads to the formation of protrusive structures. Spontaneously formed patches of F-actin in the distal axon serve as precursors to filopodial and lamellipodial extension (Fig. 5A) (Lau et al., 1999; Loudon et al., 2006). Axonal F-actin patches, thus, provide an excellent model system for investigating the dynamics of F-actin that lead to protrusive activity, and allow us to track F-actin dynamics before protrusive activity emerges. I monitored the rate of F-actin patch formation within the same axons before and after treatment with semaphorin 3A. Treatment with semaphorin 3A blocked the formation of axonal F-actin patches (Fig. 5B). These data demonstrate that semaphorin 3A shuts down the polymerization of F-actin that contributes to the formation of filopodia and lamellipodia. Inhibition of ROCK using y-27632 prevented the semaphorin-3A-induced block of F-actin-patch formation (Fig. 5B). Thus, ROCK activity in response to semaphorin 3A treatment is largely responsible for the shutdown of F-actin polymerization that leads to protrusion of filopodia and lamellipodia.

Furthermore, when patches formed in semaphorin-3A-treated axons they were much more transient than in control axons. In control axons, patches formed and proceeded to exhibit a relatively strong and localized enhanced yellow fluorescent protein (eYFP)-actin signal (Fig. 5C). However, in semaphorin-3A-treated axons, when patches formed, these signals were barely detectable and never attained similar

intensities to those of control axons (compare insets in Fig. 5C and D). Furthermore, the maximal life-span of patches observed in semaphorin-3A-treated axons was 18 seconds, less
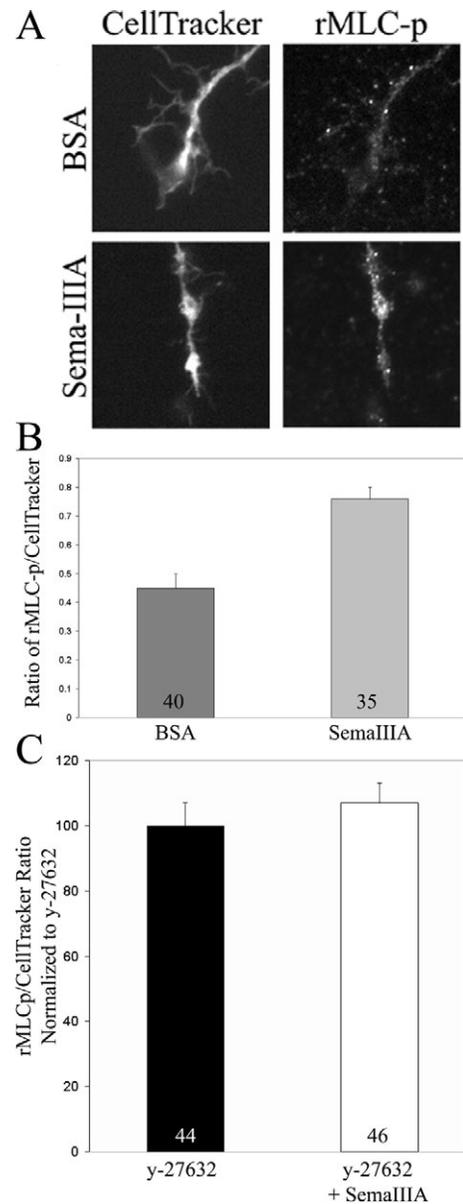

Fig. 4. Semaphorin 3A activates myosin II. (A) Neurons were loaded with 2.5 μM of the volumetric fluorescent reporter CellTracker prior to treatment with semaphorin 3A or BSA (control) for 10 minutes. Cultures were then fixed and stained with an antibody against phosphorylated regulatory myosin light chains (rMLC-p). Treatment with semaphorin 3A increased the levels of rMLC-p in axons relative to controls. (B) Quantification of the ratio of rMLC-p staining to CellTracker staining (sample size is given within bars). Semaphorin 3A increased rMLC-p staining in the distal 20 μm of the axon by 69% ($P<0.0001$, Welch t-test). The mean and s.e.m. are shown in all presentations of quantitative data. (C) Pretreatment with 10 μM y-27632 (30 minutes) prevents the semaphorin-3A-induced increase in the ratio of rMLCp to CellTracker staining ($P>0.7$, Welch t-test; sample site is givin within bars). Data are shown normalized to treatment with y-27632 alone.

than the mean duration of 23±1 seconds exhibited by patches formed before treatment with semaphorin 3A. These observations further indicate that semaphorin 3A blocks the formation of F-actin axonal patches, which serve as precursors to protrusive activity.

Inhibition of ROCK by using y-27632 blocked the effects of semaphorin 3A on the formation of eYFP-actin patches (Fig. 5B). Growth cones treated with y-27632 prior to treatment with semaphorin 3A did not collapse (compare Fig. 5D and E). Semaphorin 3A treatment reduced the size of the growth
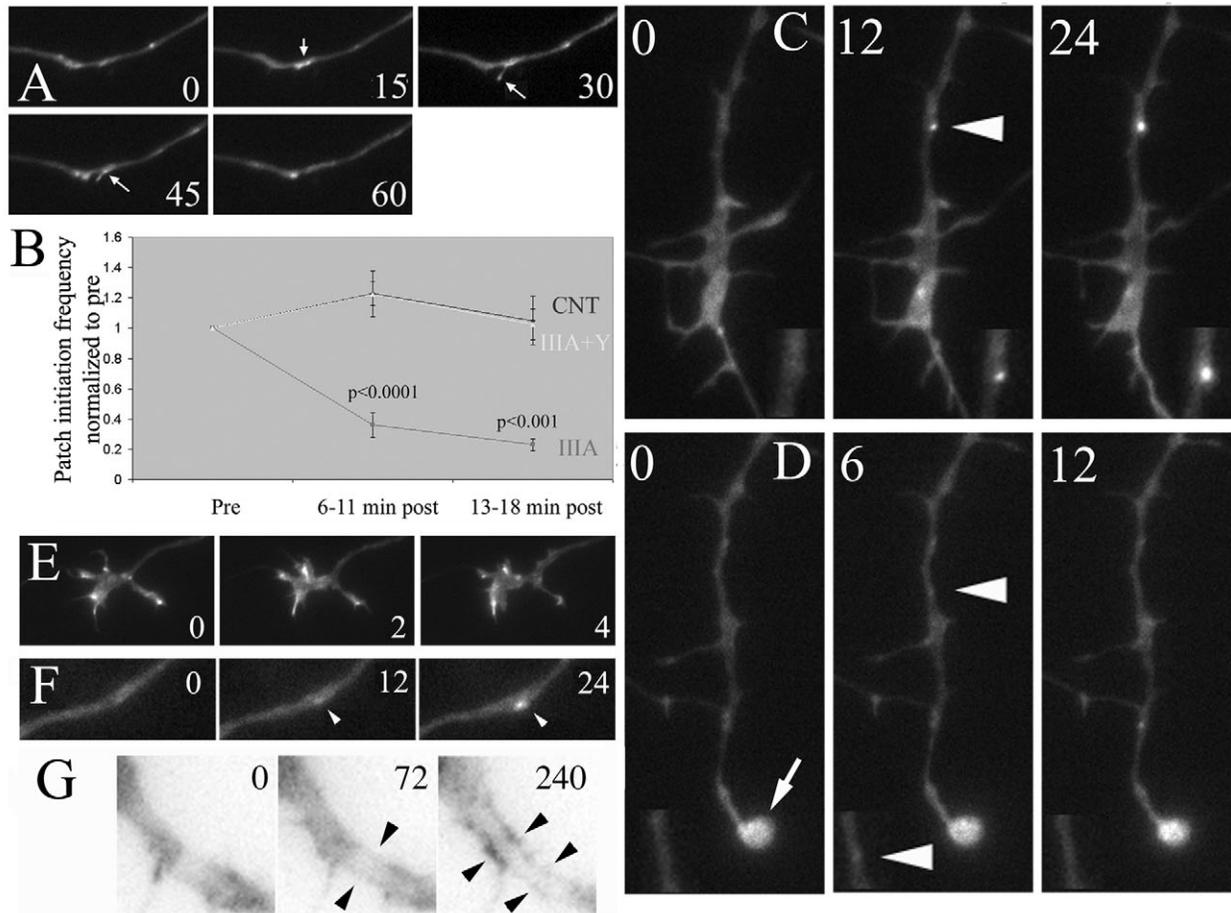

Fig. 5. Semaphorin 3A blocks the formation of axonal F-actin patches that serve as precursors to filopodial and lamellipodial extension. (A) Example of filopodial protrusion from a spontaneously formed axonal F-actin patch in an eYFP-actin expression axon. Numbers in panels reflect seconds. At 15 seconds, a patch forms (arrow) that subsequently gives rise to a filopodium (sec 30-45). By 60 seconds, the filopodium has retracted and the patch has disappeared. As described by Loudon et al., the majority of axonal protrusive events are preceded by patch formation (Loudon et al., 2006), although only approximately 6-7% of F-actin patches give rise to filopodial or lamellipodial protrusion. (B) Determination of the frequency of F-actin patch formation, during 6-minute sampling periods (6-second interframe intervals) in eYFP-actin-transfected axons revealed that semaphorin 3A inhibited the formation of patches. Inhibition of patches occurred with a similar time course to that of growth cone collapse (i.e. during the first 10 minutes of treatment). The effects of semaphorin 3A were blocked by 10 µM y-27632 (P values shown for comparison of semaphorin 3A treatment and controls within time points, Welch *t*-test, *n*=6-7 axons per group; y-27632 together with semaphorin 3A frequencies were not different from controls at either time points). (C) Example of axonal F-actin patch formation in a control axon, as previously described by Loudon et al. (Loudon et al., 2006). Patches form spontaneously and increase in size and fluorescence intensity. Double-magnification insets of the patches are shown in the bottom of each panel. Numbers in panels reflect seconds in the time-lapse sequence. Arrowhead in middle panel indicates a briefly detectable eYFP-actin patch. (D) Example of minimal patch-formation, and lack of patch development, in an axon treated with semaphorin 3A for 13 minutes. A small, but detectable, patch of eYFP-actin formed (middle panel) but the patch disappeared at 6 seconds. The rapid disappearance of patches in the semaphorin-3A-treated axon stands in contrast to the much longer live-span of patches observed in control axons (compare seconds elapsed in C and D). Arrowheads in middle panel indicate a briefly detectable eYFP-actin patch. Double-magnification insets of the patches are shown in the bottom of each panel; arrow in 0-second-panel magnification indicates the collapsed growth cone. Numbers in panels reflect seconds in the time-lapse sequence. (E) Growth cone pretreated with y-27632 followed by a 13-minute treatment with semaphorin 3A. Notice that the growth cone is not collapsed (as in D), and continues to undergo morphologic remodeling. Numbers in panels reflect minutes. (F) Example of an eYFP-actin patch (arrowhead) forming and developing in an axon pretreated with y-27632 followed by treatment with semaphorin 3A for 13 minutes. Notice the similarity to patch formation in control axons (in C). Number in panels reflect seconds. (G) Time-lapse sequence from an eYFP-actin-transfected axon treated with semaphorin 3A for 13 minutes (*t*=0); 72 seconds later, bundle-like eYFP-actin is apparent (arrowheads) and becomes more pronounced at 240 seconds. Image was inverted to increase the contrast of the eYFP-actin signal.

cone by 77±4% during the imaging period. By contrast, pretreatment with y-27632 reduced the size of the growth cone only by 23±15% following treatment with semaphorin 3A (*P*<0.01; compared with semaphorin 3A treatment alone). Furthermore, growth cones remained motile and exhibited lamellipodial and filopodial protrusion (Fig. 5E). Similarly, eYFP-actin patches that formed in axons treated with y-27632 and subsequently with semaphorin 3A, formed and developed in a manner similar to those of control axons (compare Fig. 5C and F). Thus, these data extend previous observations that inhibition of ROCK prevents growth cone collapse in growth cones of sensory neurons (Dontchev and Letourneau, 2002; Dontchev and Letourneau, 2003), by indicating that the function of ROCK is to shut down F-actin polymerization leading to protrusive activity. This is in contrast to the role of Rac1 in mediating ephrin-induced growth cone collapse, where inhibition of Rac1 does not interfere with decreasing F-actin in growth cones, although it prevents morphologic collapse (Jurney et al., 2002).

Although I have previously imaged the formation of F-actin bundles in the thin lamellipodia of growth cones by using eYFP-actin (Loudon et al., 2006), I was not able to routinely image the formation of F-actin bundles in axons due to the prevalent G-actin background–eYFP-actin–signal in the large volume of the axon shaft. In cases where I could observe bundle-like eYFP-actin signal in the axon, due to a concurrent decrease in background, the apparent bundles formed without any presaging signal or patch formation (Fig. 5G; three of seven axons).

Discussion

Axon retraction is a fundamental aspect of the response of axons to repellent guidance cues. For example, during development, inappropriately projected retinal axons undergo retraction in response to gradients of repellent guidance cues in the tectal target (Luo and O'Leary, 2005). Similarly, axons compete for space at the neuromuscular junction, and the losing axon retracts (Bernstein and Lichtman, 1999). Furthermore, retraction of the axon is an important aspect of guidance in vivo. Axons that veer off course and encounter the repellent guidance cue Slit are set back on course by retracting away from the territory expressing slit (Hutson and Chien, 2002). Elucidating the mechanism of repellent-cue-induced axon retraction is thus of great importance to understand axon guidance and the pruning of axonal pathways. In this report, I present evidence that semaphorin 3A coordinates the activation of myosin II, by generating an intra-axonal F-actin-bundle-cytoskeleton that serves as a substratum for force generation of myosin II during axonal retraction. Furthermore, I present data that imply ROCK as the downstream effector of semaphorin 3A signaling responsible for shutting down F-actin polymerization leading to protrusive activity, resulting in growth cone collapse.

Semaphorin 3A increased the levels of phosphorylated rMLC in axons in a ROCK-dependent manner, demonstrating that myosin II is activated by semaphorin 3A signaling pathways. Myosin II might be involved in growth cone collapse by generating contractile forces that could drive increased retrograde flow of F-actin in growth cones. My results are inconsistent with a role for myosin II in driving growth cone collapse in response to semaphorin 3A. However, I report that myosin II is required for semaphorin-3A-induced axon retraction. A role for myosin II in driving axon retraction would be consistent with previous demonstrations (Wylie and Chantler, 2003; Gallo et al., 2002; Gallo, 2004).

Growth cone collapse is a complex process and is not merely the consequence of F-actin depolymerization (Gallo and Letourneau, 2004). The GTPase Rac1 has been shown to be required for growth cone collapse in response to semaphorin 3A and ephrins. Interestingly, although growth cones do not collapse in response to guidance cues when Rac1 is inhibited, F-actin undergoes depolymerization to the same extent as in control growth cones treated with collapsing cues (Jurney et al., 2002). In this study, I present evidence that the shutdown of F-actin polymerization leading to protrusive activity in response to semaphorin 3A is mediated by ROCK. Semaphorin 3A blocked the formation of F-actin patches, which have been shown to be precursors to filopodial and lamellipodial protrusion (Lau et al., 1999; Loudon et al., 2006). Thus, the effects of semaphorin 3A appear to be on the earliest step in the process of protrusion, the generation of an F-actin substratum that subsequently serves to produce filopodia and lamellipodia. These data suggest that semaphorin 3A signaling inhibits F-actin nucleation, the first step in filament formation. Unfortunately, the mechanisms underlying F-actin nucleation in growth cones are largely unknown and appear to be largely independent of Arp2/3 (Strasser et al., 2004). Thus, the issue of whether semaphorin 3A directly affects proteins involved in actin nucleation will require further study. Alternatively, semaphorin 3A might not inhibit F-actin nucleation but block subsequent polymerization. These issues will require further experimental analysis.

Although ROCK is involved in the depletion of F-actin underlying protrusion of filopodia and lamellipodia, my data indicate that ROCK is also involved in the generation of axonal F-actin bundles. Thus, I suggest that ROCK acts as a major regulatory switch in the organization of F-actin in growth cones and axons downstream of semaphorin 3A signaling (Fig. 6). High levels of active ROCK shut down the generation of F-actin that contributes to protrusion but promotes the formation of F-actin bundles, which serve as a substratum for myosin-II-mediated force generation during the process of axon retraction. My data are consistent with the proposal that there are multiple cellular organizational schemes of F-actin that mediate specific cellular functions, such as protrusion and contractility (Evangelista et al., 2003). Intra-axonal F-actin bundles might represent the favored organization of F-actin for the generation of contractile forces, whereas F-actin meshworks might underlie the protrusion of the leading edge. Indeed, a current model for filopodial elongation, which is dependent on the formation of a core F-actin bundle, indicates that filopodial-bundle formation is driven by reorganization of F-actin meshworks (Svitkina et al., 2003). Furthermore, filopodial F-actin bundles are protrusive structures, unlike the intra-axonal F-actin bundles generated by semaphorin 3A. It will be of interest to further study the differences in the molecular components of filopodial and intra-axonal F-actin bundles.

To my knowledge, intra-axonal F-actin bundles have not been previously reported. Indeed, dorsal root ganglion axons extending on a laminin substratum usually exhibit very little cortical F-actin and interspersed patches of F-actin (Loudon et al., 2006). The apparent function of axonal F-actin bundles in

axonal retraction suggests that they are functionally analogous to the F-actin contractile structure of non-neuronal cells, the stress fiber. Indeed, both stress fibers and axonal F-actin bundles depend on the activity of RhoA and RhoA-kinase and generate contractile forces (Schoenwaelder and Burridge, 1999). However, stress fibers also transmit myosin-II forces onto the substratum through focal adhesions. It seems highly unlikely that this cellular function is also shared by axonal F-actin bundles. Rather, the intra-axonal cage-like organization of the bundles within the axon shaft suggests that, myosin II acting on these bundles generates forces directed either proximally along the axon towards the cell body, or centripetally towards the center of the axon. These forces would, in turn, result in the retraction of the axon, and the buckling of the axonal microtubule array due to increased compressive forces on the axonal microtubule array (Joshi et al., 1985).

Our results reveal for the first time a specific F-actin organization that is used by neurons to generate contractile forces and axon retraction. This observation suggests a solution to the paradox of myosin-II-dependent axon retraction following the loss of the richest source of F-actin, the growth cone. Guidance cues inhibit the formation of F-actin that leads to protrusion of filopodia and lamellae but promote the formation of a specialized set of intra-axonal F-actin bundles that serve as a substratum for myosin-II-dependent contractility. In this report, I demonstrate that ROCK downstream of semaphorin 3A signaling shuts down the production of F-actin patches, which serve as precursors to

protrusive activity. We have previously shown that endogenous ROCK activity inhibits baseline levels of protrusion (Loudon et al., 2006). Thus, the RhoA-ROCK signaling axis negatively controls the formation of organized F-actin involved in producing protrusive structures, while also promoting the formation of organized F-actin that leads to the generation of contractile forces. I propose that RhoA-ROCK signaling is a major determinant in the balance between cellular contractility and protrusive activity during axon extension and guidance, by coordinating myosin II activity and the organization of the F-actin cytoskeleton (Fig. 6).

Materials and Methods
Culturing
For enhanced yellow fluorescent protein (eYFP)-actin transfection experiments, dissociated embryonic-day-10 chicken dorsal root ganglion neurons were prepared and cultured as described previously (Loudon et al., 2006). For dissociation, ganglia were digested with trypsin followed by incubation in Ca^{2+}-Mg^{2+}-free saline prior to mechanical dissociation. For growth-cone-collapse- and retraction-assays, ganglia were cultured as explants. Substrata were coated overnight with 25 μg/ml laminin (Invitrogen, Carlsbad CA). Culturing was performed in defined F12H medium (Invitrogen) containing 20 ng/ml nerve growth factor (NGF; R&D Systems, Minneapolis MN).

Reagents
Semaphorin 3A was obtained from R&D Systems and kept as a stock solution at –70°C. The final concentration used in experiments was 800 ng/ml. Two hours prior to treatment with semaphorin 3A the concentration of NGF in the medium was lowered to 0.1 ng/ml to minimize growth-factor-mediated protection from growth cone collapse (Dontchev and Letourneau, 2002).

y-27632 was obtained from Calbiochem (Carlsbad, CA) and used at a final concentration of 10 μM. Purified L63RhoA and C3 proteins were purchased from Cytoskeleton Inc. (Denver, CO) and stored at –70°C at a concentration of 100 μg/ml. Blebbistatin was purchased from Toronto Research Chemicals Inc. (North York, Ontario, Canada) and a 20 mM stock solution was made in DMSO and stored at –20°C.

Peptide-mediated protein transfection
The L63RhoA and C3 proteins were delivered to cells as previously described (Gallo et al., 2002; Jurney et al., 2002). One microgram of L63RhoA, C3 or bovine serum albumin (BSA; control) was mixed with 6 μl of the cell-permeable peptide Chariot (ActiveMotif Inc., Carlsbad CA) for 30 minutes following the manufacturer's directions. For additional details on the protocol see the review by Gallo (Gallo, 2003).

eYFP-actin transfection
eYFP-actin plasmids (Clontech Inc., Palo Alto, CA) were prepared using midi-prep kits (Quiagen, Valencia, CA). Electroporation was performed using the Axama Nucleofector and reagents appropriate for chicken neurons (Amaxa, Cologne, Germany). Transfection was performed using the G013 setting of the electroporator. Ten micrograms of plasmid were used for each transfection of dissociated cells from a total of 40 ganglia. Cells were plated immediately following transfection and analyzed after one day in vitro.

Imaging
Time-lapse phase-contrast imaging of cultures was performed with a Zeiss Axiovert 135M microscope (Zeiss Inc., Göttingen, Germany), equipped with a Zeiss AxioCam CCD camera. Illumination was provided by a 100 W halogen system at minimal strength controlled by the built-in illumination-intensity controller. The stage was heated by an air curtain (ASI 400; Nevtek, Burnsville VA). Time-lapse fluorescence imaging was performed using a fully motorized Zeiss 200M inverted microscope with a Zeiss three-plate insert heated-stage and equipped with an Orca ER CCD camera (Hamamatsu Inc, Bridgewater, NJ). All fluorescence-imaging data acquisition and analysis were performed using Zeiss AxioVision software. 20× and 100× objectives (Zeiss) were used for phase- and fluorescence-microscopy, respectively. eYFP-actin patch formation was determined as described by Loudon et al. (Loudon et al., 2006). Imaging was performed using minimal light from a 100 W mercury source by closing the aperture diaphragm, and 200 millisecond to 300-millisecond exposures with 2×2 pixel binning. Images were acquired using 6-second interframe intervals. Time-lapse sequences were analyzed using Zeiss AxioVision Software.

Immunocytochemistry
Cells grown on coverslips were fixed with 0.25% glutaraldehyde for 15 minutes,
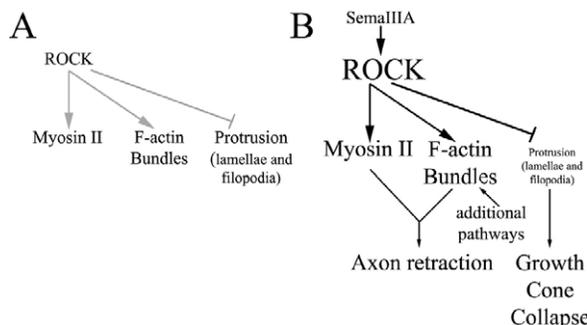

Fig. 6. Model of the proposed role of RhoA-kinase (ROCK) in the coordinated regulation of the axonal F-actin cytoskeleton and myosin II activity in response to semaphorin 3A signaling. (A) Under normal conditions, RhoA-kinase (ROCK) activity is low. However, as previously reported (Loudon et al., 2006), endogenous baseline-ROCK-activity contributes to the negative regulation of protrusion, and promotes myosin II activity and the formation of a population of F-actin bundles in growth cones. (B) Following activation of RhoA by semaphorin 3A, ROCK activity is elevated, resulting in the suppression of protrusive activity, which contributes to growth cone collapse. In concert, elevated ROCK activity promotes the activation of myosin II and the formation of non-protrusive intra-axonal F-actin bundles that serve as a substratum for myosin II to generate the contractile forces required to drive axon retraction. Since inhibition of ROCK only partially blocked the formation of axonal bundles, additional pathways not elucidated in this report probably contribute to bundle formation. This diagram shows the proposed map of ROCK–myosin-II functions in growth cone collapse and axon retraction induced by semaphorin 3A. Since growth cone collapse occurs before axon retraction, the time course of the functions of ROCK–myosin-II in these two processes is not directly shown here.

washed and treated with sodium borohydride (2 mg/ml) for 15 minutes. Cells were then blocked and permeabilized with 10% goat serum in phosphate buffered saline containing 0.1% Triton X-100 (GST). F-actin was detected with phalloidin (Molecular Probes, Eugene, OR). Myosin IIA and myosin IIB were detected using isoform-specific antibodies from Covance (Berkeley, CA) at dilution 1:200. Coverslips were double-labeled for F-actin and either myosin IIA or myosin IIB. The labeling pattern of both myosin II antibodies was detected using the same Rhodamine-labeled secondary antibody (Jackson Immunoresearch Laboratories, West Grove, PA; 1:400). Primary and secondary antibodies were applied in GST. Omission of the primary antibody resulted in no detectable staining. Coverslips were mounted in nofade medium and stored at –20°C until analysis.

For detection of phosphorylated regulatory myosin light chains, I used an affinity-purified antibody raised against chicken light chains phosphorylated on serine residue 19 (gift of H. F. Yee, UCSF, CA), the major site of phosphorylation on light chains by myosin light chain kinase and RhoA-kinase (Bresnick, 1999). The methods were essentially as previously reported (Loudon et al., 2006). Briefly, prior to experimentation and fixation, axons were loaded with the cell-permeable aldehyde-fixable volumetric marker CellTracker (2.5 μM; Molecular Probes) for 30 minutes, followed by washing with medium. Coverslips were fixed using 4% paraformaldehyde and stained with the light-chain antibody (dilution 1:1000) overnight at 4°C, as previously described. Coverslips were then labeled with 1:200 goat-anti rabbit secondary antibody conjugated to Rhodamine (Jackson). Ratiometric determination of the levels of light-chain staining relative to CellTracker were performed as previously described (Loudon et al., 2006). Briefly, the relative mean intensities in defined areas of interest were measured using AxioVision software, while making sure that the signal was below saturation in all channels, under all experimental conditions. Staining intensities were determined in the distal 20 μm of axons.

References

Ahmad, F. J., Hughey, J., Wittmann, T., Hyman, A., Greaser, M. and Baas, P. W. (2000). Motor proteins regulate force interactions between microtubules and microfilaments in the axon. *Nat. Cell Biol.* **2**, 276-280.

Aizawa, H., Wakatsuki, S., Ishii, A., Moriyama, K., Sasaki, Y., Ohashi, K., Sekine-Aizawa, Y., Sehara-Fujisawa, A., Mizuno, K., Goshima, Y. et al. (2001). Phosphorylation of cofilin by LIM-kinase is necessary for semaphorin 3A-induced growth cone collapse. *Nat. Neurosci.* **4**, 367-373.

Alabed, Y. Z., Grados-Munro, E., Ferraro, G. B., Hsieh, S. H. and Fournier, A. E. (2006). Neuronal responses to myelin are mediated by rho kinase. *J. Neurochem.* **96**, 1616-1625.

Bernstein, M. and Lichtman, J. W. (1999). Axonal atrophy: the retraction reaction. *Curr. Opin. Neurobiol.* **9**, 364-370.

Bresnick, A. R. (1999). Molecular mechanisms of nonmuscle myosin-II regulation. *Curr. Opin. Cell Biol.* **11**, 26-33.

Bridgman, P. C. (2002). Growth cones contain myosin II bipolar filament arrays. *Cell Motil. Cytoskeleton* **52**, 91-96.

Bridgman, P. C., Dave, S., Asnes, C. F., Tullio, A. N. and Adelstein, R. S. (2001). Myosin IIB is required for growth cone motility. *J. Neurosci.* **21**, 6159-6169.

Burridge, K. and Chrzanowska-Wodnicka, M. (1996). Focal adhesions, contractility, and signaling. *Annu. Rev. Cell Dev. Biol* **12**, 463-518.

Dontchev, V. D. and Letourneau, P. C. (2002). Nerve growth factor and semaphorin 3A signaling pathways interact in regulating sensory neuronal growth cone motility. *J. Neurosci.* **22**, 6659-6669.

Dontchev, V. D. and Letourneau, P. C. (2003). Growth cones integrate signaling from multiple guidance cues. *J. Histochem. Cytochem.* **51**, 435-444.

Evangelista, M., Zigmond, S. and Boone, C. (2003). Formins: signaling effectors for assembly and polarization of actin filaments. *J. Cell Sci.* **116**, 2603-2611.

Gallo, G. (2003). Making proteins into drugs: assisted delivery of proteins and peptides into living neurons. *Methods Cell Biol.* **71**, 325-338.

Gallo, G. (2004). Myosin II activity is required for severing-induced axon retraction in vitro. *Exp. Neurol.* **189**, 112-121.

Gallo, G. and Letourneau, P. C. (2004). Regulation of growth cone actin filaments by guidance cues. *J. Neurobiol.* **58**, 92-102.

Gallo, G., Yee, H. F., Jr, and Letourneau, P. C. (2002). Actin turnover is required to prevent axon retraction driven by endogenous actomyosin contractility. *J. Cell Biol.* **158**, 1219-1228.

Gehler, S., Shaw, A. E., Sarmiere, P. D., Bamburg, J. R. and Letourneau, P. C. (2004). Brain-derived neurotrophic factor regulation of retinal growth cone filopodial dynamics is mediated through actin depolymerizing factor/cofilin. *J. Neurosci.* **24**, 10741-10749.

Guha, M., Zhou, M. and Wang, Y. L. (2005). Cortical actin turnover during cytokinesis requires myosin II. *Curr. Biol.* **15**, 732-736.

Hall, C., Brown, M., Jacobs, T., Ferrari, G., Cann, N., Teo, M., Monfries, C. and Lim, L. (2001). Collapsin response mediator protein switches RhoA and Rac1 morphology in N1E-115 neuroblastoma cells and is regulated by Rho kinase. *J. Biol. Chem.* **276**, 43482-43486.

Hu, H., Marton, T. F. and Goodman, C. S. (2001). Plexin B mediates axon guidance in Drosophila by simultaneously inhibiting active Rac and enhancing RhoA signaling. *Neuron* **32**, 39-51.

Hutson, L. D. and Chien, C. B. (2002). Pathfinding and error correction by retinal axons: the role of astray/robo2. *Neuron* **33**, 205-217.

Jurney, W. M., Gallo, G., Letourneau, P. C. and McLoon, S. C. (2002). Rac1-mediated endocytosis during ephrin-A2- and semaphorin 3A-induced growth cone collapse. *J. Neurosci.* **22**, 6019-6028.

Joshi, H. C., Chu, D., Buxbaum, R. E. and Heidemann, S. R. (1985). Tension and compression in the cytoskeleton of PC 12 neurites. *J. Cell Biol.* **101**, 697-705.

Kolega, J. (2004). Phototoxicity and photoinactivation of blebbistatin in UV and visible light. *Biochem. Biophys. Res. Commun.* **320**,1020-1025.

Lau, P. M., Zucker, R. S. and Bentley, D. (1999). Induction of filopodia by direct local elevation of intracellular calcium ion concentration. *J. Cell Biol.* **145**, 1265-1275.

Letourneau, P. C. (1983). Differences in the organization of actin in the growth cones compared with the neurites of cultured neurons from chick embryos. *J. Cell Biol.* **97**, 963-973.

Loudon, R., Silver, L., Yee, H. F., Jr and Gallo, G. (2006). RhoA-kinase and myosin II are required for the maintenance of growth cone polarity and guidance by nerve growth factor. *J. Neurobiol.* **66**, 847-867.

Luo, L. and O'Leary, D. D. (2005). Axon retraction and degeneration in development and disease. *Annu. Rev. Neurosci.* **28**, 127-156.

Maupin, P. and Pollard, T. D. (1986). Arrangement of actin filaments and myosin-like filaments in the contractile ring and of actin-like filaments in the mitotic spindle of dividing HeLa cells. *J. Ultrastruct. Mol. Struct. Res.* **94**, 92-103.

Plachez, C. and Richards, L. J. (2005). Mechanisms of axon guidance in the developing nervous system. *Curr. Top. Dev. Biol.* **69**, 267-346.

Rochlin, M. W., Itoh, K., Adelstein, R. S. and Bridgman, P. C. (1995). Localization of myosin II A and B isoforms in cultured neurons. *J. Cell Sci.* **108**, 3661-3670.

Schoenwaelder, S. M. and Burridge, K. (1999). Bidirectional signaling between the cytoskeleton and integrins. *Curr. Opin. Cell Biol.* **11**, 274-286.

Solomon, F. and Magendantz, M. (1981). Cytochalasin separates microtubule disassembly from loss of asymmetric morphology. *J. Cell Biol.* **89**, 157-161.

Straight, A. F., Cheung, A., Limouze, J., Chen, I., Westwood, N. J., Sellers, J. R. and Mitchison, T. J. (2003). Dissecting temporal and spatial control of cytokinesis with a myosin II Inhibitor. *Science* **299**, 1743-1747.

Strasser, G. A., Rahim, N. A., VanderWaal, K. E., Gertler, F. B. and Lanier, L. M. (2004). Arp2/3 is a negative regulator of growth cone translocation. *Neuron* **43**, 81-94.

Svitkina, T. M., Bulanova, E. A., Chaga, O. Y., Vignjevic, D. M., Kojima, S., Vasiliev, J. M. and Borisy, G. G. (2003). Mechanism of filopodia initiation by reorganization of a dendritic network. *J. Cell Biol.* **160**, 409-421.

Swiercz, J. M., Kuner, R., Behrens, J. and Offermanns, S. (2002). Plexin-B1 directly interacts with PDZ-RhoGEF/LARG to regulate RhoA and growth cone morphology. *Neuron* **35**, 51-63.

Turney, S. G. and Bridgman, P. C. (2005). Laminin stimulates and guides axonal outgrowth via growth cone myosin II activity. *Nat. Neurosci.* **8**,717-719.

Ueda, K., Murata-Hori, M., Tatsuka, M. and Hosoya, H. (2002). Rho-kinase contributes to diphosphorylation of myosin II regulatory light chain in nonmuscle cells. *Oncogene* **21**, 5852-5860.

Wahl, S., Barth, H., Ciossek, T., Aktories, K. and Mueller, B. K. (2000). Ephrin-A5 induces collapse of growth cones by activating Rho and Rho kinase. *J. Cell Biol.* **149**, 263-270.

Watanabe, N., Kato, T., Fujita, A., Ishizaki, T. and Narumiya, S. (1999). Cooperation between mDia1 and ROCK in Rho-induced actin reorganization. *Nat. Cell Biol.* **1**, 136-143.

Wu, K. Y., Hengst, U., Cox, L. J., Macosko, E. Z., Jeromin, A., Urquhart, E. R. and Jaffrey, S. R. (2005). Local translation of RhoA regulates growth cone collapse. *Nature* **436**, 1020-1024.

Wylie, S. R. and Chantler, P. D. (2003). Myosin IIA drives neurite retraction. *Mol. Biol. Cell* **14**, 4654-4666.

Yoneda, A., Multhaupt, H. A. and Couchman, J. R. (2005). The Rho kinases I and II regulate different aspects of myosin II activity. *J. Cell Biol.* **170**, 443-453.